

UDC 544.52

SILVER AZIDE PHOTOLYSIS

E.P. Surovoy, S.M. Sirik, L.N. Bugerko

Kemerovo State University
E-mail: epsur@kemsu.ru

The preliminary silver azide light irradiation ($\lambda=365$ nm, $I>1\cdot 10^{15}$ quanta \cdot cm $^{-2}\cdot$ c $^{-1}$) in vacuum ($P=1\cdot 10^{-5}$ Pa) alongside with increase in photolysis speed and a photocurrent results in occurrence new long-wave (up to $\lambda=1280$ nm) area of spectral sensitivity. Constants of silver azide photolysis speed are determined. As a result of measurements of a contact potential difference, volt – ampere of characteristics, a contact photoelectrical moving force, a photocurrent it is established, that at silver azide photolysis microheterogeneous systems AgN_3 (A_1) – Ag (a product photolysis) are formed. It is shown, that a limiting stage of silver azide photolysis is diffusion of the mobile ion of silver to neutral center ($T_r\text{Ag}_m$)^o.

The solid-phase products, extracted at decomposition, influence significantly photochemical and photoelectric properties of heavy metals azides [1–5]. The investigation of autocatalytic and sensitizing influence of solid-phase products on azides photolysis [6–8], as well as parallel study of the photolysis and electrophysical properties of azid-metal (azid-semiconductor) heterosystems [9–18] allowed advancing significantly in the direction of understanding the photolysis mechanism of inorganic azides at deep once-through conversion. In the given paper the results of the work directed on the investigation of kinetic and spectral regularities of products formation in the process of silver azide photolysis, depending on incident light intensity, ascertainment of energy structure of silver azide contact – the photolysis product and causes, resulting in observed changes of photochemical and photoelectric sensitivity of silver azide with the product of decomposition are presented.

Objects and methods of investigation

Silver azide of A_1 ($\text{AgN}_3(A_1)$) type was synthesized by the method of two-jet crystallization (0,2 n water solution of doubly recrystallized technical sodium azide was instilled to 0,2 n water solution of silver nitrate (of the qualification ch.p.)). The rate of instillation was 2 drops per minute, $\tau_{\text{synthesis}}=30$ min., $T=293$ K, pH 3. Silver azide of B_1, B_2, B_3 ($\text{AgN}_3(B_1, B_2, B_3, B_{1a}, B_{2a}, B_{2b})$) type was synthesized by the method of two-jet crystallization instilling, at the speed of $7\cdot 10^{-4}$ mole \cdot min $^{-1}$, water 0,2 N solutions of silver nitrate (of the qualification ch.p.) and doubly recrystallized technical potassium azide into mother 0,1 N waters (the rate of instillation was $7\cdot 10^{-3}$ mole \cdot min $^{-1}$ – B_{1a}), 0,2 N (in the presence of

0,006 g and 0,02 g of neonol – syntheses B_{2a}, B_{2b} respectively) and 0,3 N solution of potassium nitrate (of the qualification ch.p.) $\tau_{\text{synthesis}}=6,5$ min, $T=293$ K, pH 6. The samples for investigations were prepared by pressing tablets $\text{AgN}_3(A_1)$ with the weight 125 mg at pressure $4\cdot 10^3$ kg \cdot sm $^{-2}$, or by means of thorough dispersion of a $\text{AgN}_3(A_1)$ portion of the weight 125 mg in water, further overall spreading (by the method of coating) into bowls with the diameter of 1 sm and were dried in the exiccator in the dark at 293 K [6, 9]. Photolysis velocity V_f , photocurrent i_{ph} and photo-emf U_{ph} of the samples were measured at pressure $\sim 1\cdot 10^{-5}$ Pa. Mercury (DRT-250) and xenon (DKsSh-1000) lamps were light sources. Monochromator MSD-1 and optical filters set were applied for extraction the required spectral region. Actinometry of light sources was carried out by means of radiation thermocouple RT-0589. The lamp RMO-4S of Omegatron mass-spectrometer IPDO-1, adjusted to the frequency of nitrogen recording, was used as a sensor at V_{ph} measurement [12]. I_{ph} and U_{ph} measurements were carried out at the device, including electrometric voltmeter V7-30, or electrometer TR-1501 [15]. Diffuse reflection spectrum (DR), before and after samples irradiation, were measured at pressure $\sim 10^{-4}$ Pa, using the device [16], at spectrophotometer SPh-4A with the attachment PDO-1 at pressure 101,3 kPa, at spectrophotometer Specord-M40 equipped with 8^od reflection [17]. Contact potential difference (CPD) between silver azide, silver and platinum reference electrode was measured, using the modified method of Kelvin [19]. The topography of solid-phase products of lead azide photolysis was studied by the method of carbon replica at electron microscope UEMV-1000.

Results and discussion

The kinetic curves of V_{ph} $AgN_3(A_1)$ at the influence on light samples from the area of lead azide fundamental absorption ($\lambda=365$ nm) at 293 K in the range of intensities of incident light $I=3,06 \cdot 10^{16} \dots 8,56 \cdot 10^{13} \text{ sm}^{-2} \cdot \text{s}^{-1}$ are presented in Fig. 1. In the fields of intensive lightning ($I > 1 \cdot 10^{15} \text{ quantum} \cdot \text{sm}^{-2} \cdot \text{s}^{-1}$) on kinetic curves of V_{ph} several areas may be distinguished: initial (I), stationary (II), rise (III), saturation (IV). The decrease of incident light intensity results in reduction of V_{ph} as well as increase of kinetic curves area length. The velocity of silver azide photolysis and realization time of different areas of V_{ph} kinetic curves depends, to a considerable degree, on the way of preparations synthesis (Fig. 2).

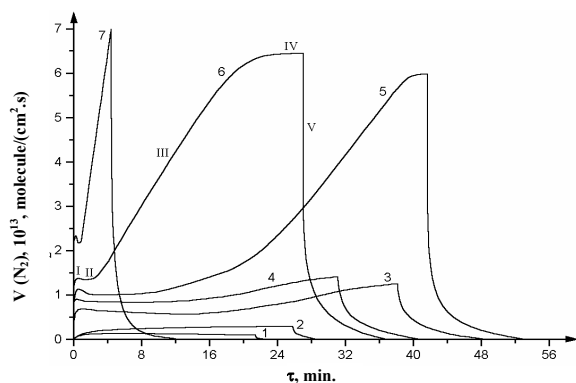


Fig. 1. Dependence of photolysis velocity of $AgN_3(A_1)$ on incident light intensity (I , $\text{quantum} \cdot \text{sm}^{-2} \cdot \text{s}^{-1}$) $\lambda=365$ nm: 1) $8,56 \cdot 10^{13}$, 2) $2,42 \cdot 10^{14}$, 3) $8,4 \cdot 10^{14}$, 4) $2,42 \cdot 10^{15}$, 5) $3,17 \cdot 10^{15}$, 6) $6,5 \cdot 10^{15}$, 7) $3,06 \cdot 10^{16}$

Spectral distributions of V_{ph} and i_{ph} , plotted by stationary magnitudes of V_{ph} and i_{ph} are presented in Fig. 3 (curves 1, 2). It is seen that the long-wave edge of V_{ph} and

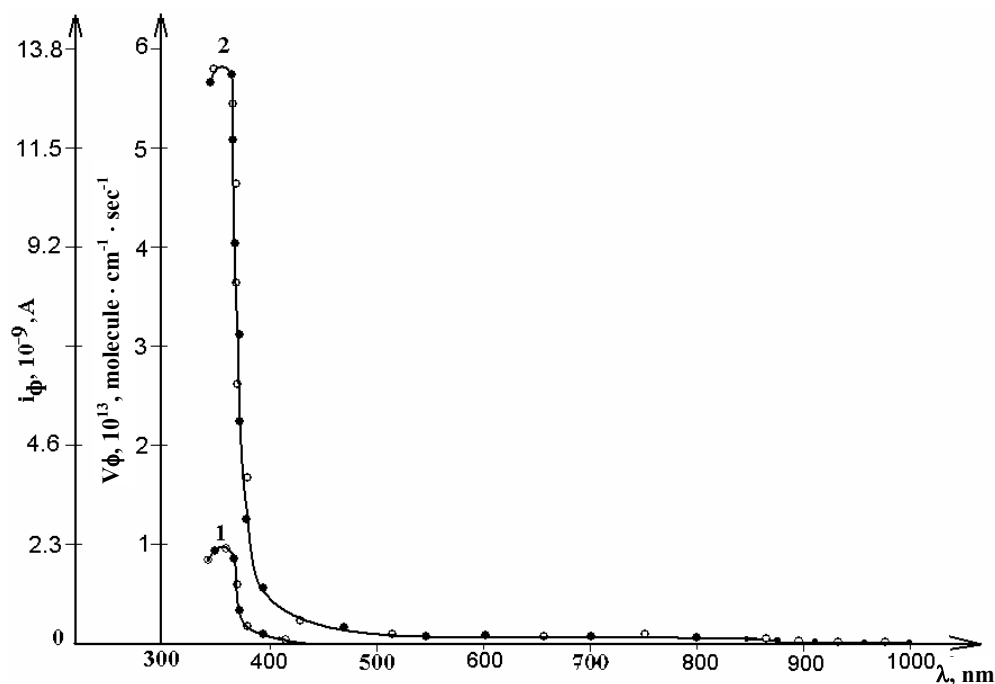


Fig. 3. Spectral distribution of photolysis (0), photocurrent(O) velocity before (•) and after irradiation of $AgN_3(A_1)$ (2) with light $\lambda=365$ nm at $I=3,17 \cdot 10^{15} \text{ quantum} \cdot \text{sm}^{-2} \cdot \text{s}^{-1}$

i_{ph} $AgN_3(A_1)$ is at $\lambda \approx 365$ nm. Various types of pretreatments, which result in partial decomposition of silver azide (heating at pressure $\sim 10^{-5}$ Pa in temperature range between 340...420 K, irradiation with light, samples ageing, treatment in reducing medium), decrease or fully remove the initial maximum (area I) on kinetic curves of V_{ph} . The repeated (after light breaking at I and II areas) samples lightning does not result in significant change of V_{ph} at II, III, IV areas of the kinetic curves of V_{ph} (Fig. 4, curves 2,3) and curves of spectral distribution of V_{ph} and i_{ph} (Fig. 3). The preexposure of the samples during 40 minutes results in monotonic increase of V_{ph} to the constant magnitudes (Fig.4, curve 4). In this case, alongside with V_{ph} and i_{ph} increase in their own absorbing region of $AgN_3(A_1)$ on the curves of spectral distribution of V_{ph} and i_{ph} , the new region of photosensitivity, the long-wave edge of which spreads to 1280 nm, appears (Fig. 3, curves 3,4).

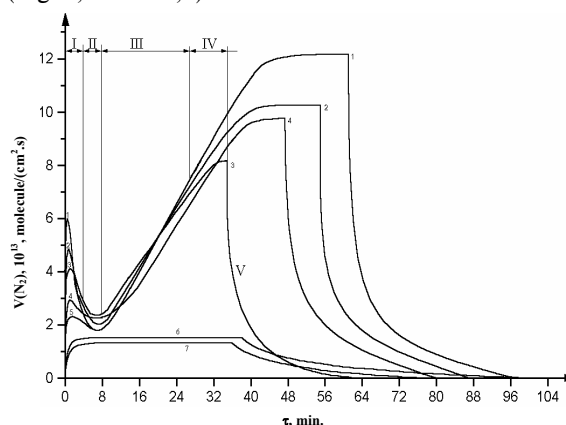


Fig. 2. Dependence of velocity of silver azide photolysis on the method of synthesis at $\lambda=365$ nm, $I=3,17 \cdot 10^{15} \text{ quantum} \cdot \text{sm}^{-2} \cdot \text{s}^{-1}$: 1) B_1 , 2) B_2 , 3) B_3 , 4) A_1 , 5) B_{1a} , 6) B_{2a} , 7) B_{2a}

Longer lightning of the samples causes V_{ph} decrease. In the issue of electron microscopic and spectrophotometric investigations, it was stated that the observed decrease of $AgN_3(A_1)$ photosensitivity is connected with blackout of sample surface with solid phase product of photolysis and, as a result, with the decrease of a number of absorbed light quanta by $AgN_3(A_1)$.

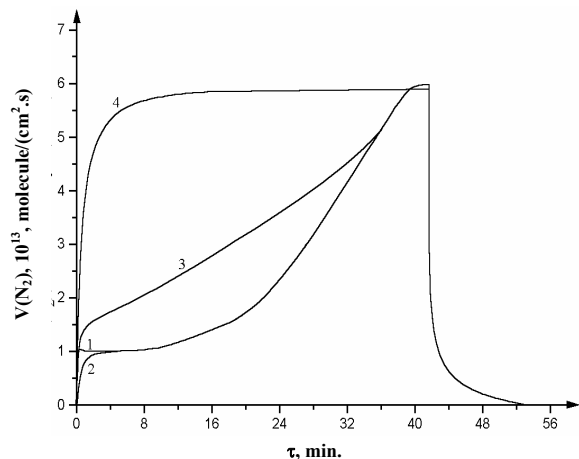


Fig. 4. Kinetic curves of $AgN_3(A_1)$ photolysis rate at $\lambda=365$ nm and incident light intensity $I=3,17 \cdot 10^{15}$ quantum \cdot sm $^{-2}\cdot$ s $^{-1}$ before (1) and after lightning breaking at I (2), II (3), IV (4) areas of V_{ph} kinetic curves

After the end of exposure at different areas of the kinetic curves of photolysis rate the region of a dark post gas release is observed (Fig. 1, 2, 4). It is seen that the curves of dark post gas release consist of two areas «fast» and «slow». The duration of the dark post gas release increases with the growth of exposure time and incident light intensity. And the time interval of «slow» constituent in the dark post gas release decreases at falling temperature and incident light intensity. It is stated that the curves of the dark post gas release are rectified in coordinates $\ln C_{N_2}=f(\tau)$ independently of incident light intensity and preexposure time. The values of rate constants (k) after lightning breaking at different areas of V_{ph} kinetic curves were estimated by slope ratio of $\ln C_{N_2}=a(\tau)$ dependence (Table 1).

Table 1. Rate constants of the process, responsible for post gas release k , s $^{-1}$

Sample	Areas of kinetic curve of V_{ph}		
	I	II	IV
$AgN_3(A_1)$	$(4,32 \cdot 0,16) \cdot 10^{-2}$	$(3,10 \cdot 0,15) \cdot 10^{-2}$	$(2,40 \cdot 0,12) \cdot 10^{-3}$

Investigating the topography of solid phase product of silver azide photolysis, it was stated that at irradiation with light $\lambda=365$ nm, intensity $I=4 \cdot 10^{14} \dots 8 \cdot 10^{15}$ quantum \cdot sm $^{-2}\cdot$ s $^{-1}$ and times of samples irradiation, corresponding to obtaining areas I and II of V_{ph} kinetic curve, particles of two sizes mainly $d \approx 35 \dots 40$ Å и $d \approx 100 \dots 120$ Å of spherical form are formed. At $AgN_3(A_1)$ exposure to the area III the particles of solid phase product achieve the size of $\approx 0,1$ mkm and obtain faceting. At irradiation times, corresponding to the obtaining of area IV, the $AgN_3(A_1)$ surface is covered practically fully with solid phase product.

The long-wave DR edge of silver azide is at $\lambda=365$ nm (Fig. 5). Samples treatment with light $\lambda=365$ nm in the range of intensities $I=3,77 \cdot 10^{14} \dots 6,62 \cdot 10^{15}$ quantum \cdot sm $^{-2}\cdot$ s $^{-1}$, along with absence of noticeable effects in proper area of silver azide absorption, results in significant change of spectral curves mode of DR in the field of $\lambda \geq 365$ nm. At irradiation times, corresponding to I and II areas realization on V_{ph} kinetic curves, together with DR decrease in the range of $\lambda \geq 365$ nm on DR spectral curves, broad bands with maximums at $\lambda \approx 420$ and 600 nm appear. Further time increase of light treatment to the area (III) results in bands broadening and maximums shift into the long-wave region of spectrum. The results of comparison of areas graphic charts, corresponding to the change of samples reflectance at various times and intensities of exposure and calculated by DR spectra, from irradiation time with kinetic curves to photolytic silver formation, are presented in Fig. 6. The coincidence of kinetic dependences of photolytic metal (C_{Me}) quantity change, calculated by the results of measurements of V_{ph} kinetic curves at different incident light intensities, with areas (S) values, corresponding to $AgN_3(A_1)$ DR change in the process of irradiation was stated.

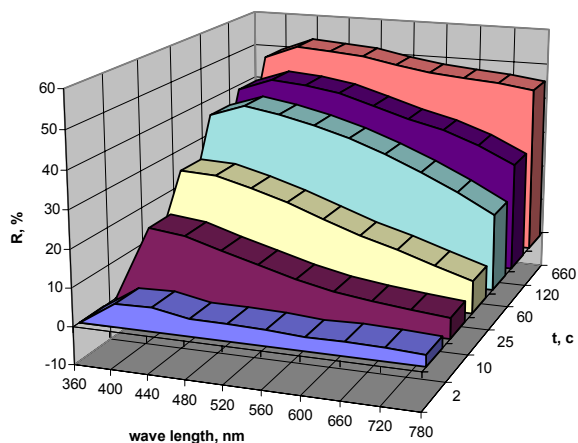


Fig. 5. Change of $AgN_3(A_1)$ reflectance depending on irradiation time with light $\lambda=365$ nm and at $I=3,17 \cdot 10^{15}$ quantum \cdot sm $^{-2}\cdot$ s $^{-1}$

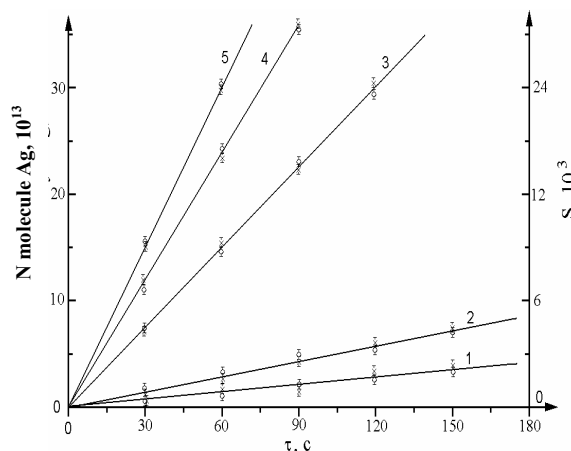


Fig. 6. Comparison of photolytic silver quantity (N) (crosses) and areas, corresponding to reflectance change (circles) on irradiation time of $AgN_3(A_1)$ with light $\lambda=365$ nm at I , quantum \cdot sm $^{-2}\cdot$ s $^{-1}$: 1) $8,56 \cdot 10^{13}$; 2) $2,42 \cdot 10^{14}$; 3) $8,4 \cdot 10^{14}$; 4) $2,42 \cdot 10^{15}$; 5) $3,17 \cdot 10^{15}$

Rate constants of $\text{AgN}_3(\text{A}_1)$ photolysis and accumulation of silver particles of proper sizes, estimated by slope ratio of dependences $\ln S = f(\tau)$ and $\ln C_{\text{Me}} = f(\tau)$ are given in Table 2.

Table 2. Rate constants of $\text{AgN}_3(\text{A}_1)$ photolysis and accumulation of silver particles (k), calculated by kinetic curves of photolysis rate (k_{ph}) and spectra of diffuse reflection (k_{DR})

I , quantum- $\text{sm}^{-2} \cdot \text{s}^{-1}$	$k_{\text{ph}} \cdot 10^2$, s^{-1}	$k_{\text{DR}} \cdot 10^2$, s^{-1}	k , s^{-1} ($d \approx 35 \dots 40 \text{ \AA}$) \times $\times 10^3$, s^{-1}	k , s^{-1} ($d \approx 100 \dots 120 \text{ \AA}$) \times $\times 10^3$, s^{-1}
$2,8 \cdot 10^{14}$	$1,1 \pm 0,2$	$1,2 \pm 0,1$	$1,2 \pm 0,2$	$2,0 \pm 0,3$
$1,6 \cdot 10^{15}$	$1,9 \pm 0,3$	$2,0 \pm 0,2$	$1,1 \pm 0,1$	$2,10 \pm 0,1$
$2,6 \cdot 10^{15}$	$3,3 \pm 0,2$	$3,5 \pm 0,3$	$1,2 \pm 0,1$	$2,30 \pm 0,2$
$3,17 \cdot 10^{15}$	$4,5 \pm 0,4$	$4,8 \pm 0,5$	$2,1 \pm 0,2$	$3,90 \pm 0,5$

The data obtained in this paper and before [15–18] indicate that, first of all, the main products of $\text{AgN}_3(\text{A}_1)$ photolysis in high vacuum environment are metallic silver and gaseous nitrogen. Besides, products of $\text{AgN}_3(\text{A}_1)$ photolysis are formed in stoichiometric ratio and, generally, on samples surface. And changes on V_{ph} kinetic curves, spectral distribution curves of V_{ph} and i_{ph} and spectral curves of $\text{AgN}_3(\text{A}_1)$ DR (Fig. 5), observed as a result of light influence, are specified by silver particles formation, and broad bands with maximums at $\lambda \approx 420$ and 600 nm – with silver particles formation mainly of average size $d \approx 35 \dots 40 \text{ \AA}$ and $d \approx 100 \dots 120 \text{ \AA}$.

To ascertain the mechanism of silver influence on silver azide photolysis the voltage-current characteristics (VCC), heterosystems U_{ph} of $\text{AgN}_3(\text{A}_1) - \text{Ag}$ (the product of photolysis) and CPD were measured.

Table 3. Contact potential difference between silver azide, silver and relative platinum electrode

Sample	CPD, V				
	Pressure, Pa				
	$1 \cdot 10^5$	$1 \cdot 10^{-5}$	$1 \cdot 10^{-5**}$	$1 \cdot 10^{-5***}$	$1 \cdot 10^{-5***}$
$\text{AgN}_3(\text{A}_1)$	+0,54	+0,52	+0,30	+0,40	+0,41
Ag	+0,40	+0,40	+0,41		

* After thermal pretreatment at 350 K during 90 min

** After preliminary thermolysis at 550 K during 180 min

*** After preliminary photolysis at $\lambda = 365 \text{ nm}$, $I = 1 \cdot 10^{14}$ quantum- $\text{sm}^{-2} \cdot \text{s}^{-1}$ during 90 min

It is seen from Table 3 that $\text{AgN}_3(\text{A}_1)$ photolysis results in decreasing CPD values, and CPD values for the samples, subjected to photolysis, coincide satisfactorily with those, measured for synthetically applied silver [19]. It was stated from VAC analysis and the results of CPD measurements that in contact region of $\text{AgN}_3(\text{A}_1) - \text{Ag}$ (due to unconformity between work functions from contact partners) a barrier electrical layer appears – $\text{AgN}_3(\text{A}_1) - \text{Ag}$ contact displays straighten properties. It is evident from Fig. 3 that U_{ph} polarity corresponds to positive sign from the side of silver azide, being constant along whole spectrum, and spectral distribution curves of U_{ph} , V_{ph} , i_{ph} correlate with each other. U_{ph} generation indicates directly about formation of microheterogeneous systems $\text{AgN}_3(\text{A}_1) - \text{Ag}$ in the process of $\text{AgN}_3(\text{A}_1)$ photolysis, dark and photoprocesses on the boundary of which, pro-

bably, provide the increase of V_{ph} and i_{ph} in proper absorbing region of silver azide (Fig. 3, 4) as well as new long-wave areas of photosensitivity appearance (Fig. 3).

Photochemical developments of photoelectric processes in such systems may be caused by redistribution of charged carriers generated by light under the influence of contact region [6–9, 15–18]. These processes lead to significant changes of photolysis conditions in preliminarily photodecomposed preparations of silver azide in comparison with photodecomposition of makeup ones. The diagram of energy bands of $\text{AgN}_3(\text{A}_1) - \text{Ag}$ contact is presented in Fig. 7. The results of CPD measurements, VAC, data on spectral distribution of U_{ph} , V_{ph} and i_{ph} , as well as the results of extrinsic photoeffect measurements were used in plotting this diagram. [20].

The intensive generation of electron-hole pairs occurs at light influence from proper absorption region of silver azide (Fig. 7, junction 1).

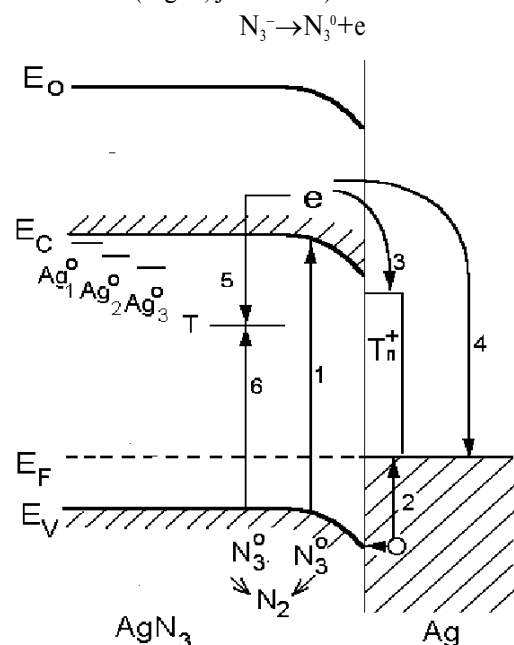


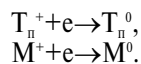
Fig. 7. Diagram of energy bands of $\text{AgN}_3(\text{A}_1) - \text{Ag}$ heterosystem, E_V – is the valence band top, E_C is the bottom of conduction band, E_F is the Fermi level, E_0 is the vacuum level, T is the combination centre

As quantum yield of photolysis, estimated by the initial piece of V_{ph} kinetic curve, makes $0,002 \dots 0,01$, then a part of photoinduced carriers of a charge is recombined (Fig. 7, junctions 5, 6)



where T^+ is the centre of recombination.

Pair of carriers, generated in the region of $\text{AgN}_3(\text{A}_1)$ space charge, are redistributed in a contact field, formed due to unconformity between the thermionic work functions of silver azide and photolytic silver and presence of proper surface electron states (PSES) [19], with transition of nonequilibrium electrons from $\text{AgN}_3(\text{A}_1)$ conduction band to the levels of PSES (T_s^+) or directly into metal (M^+) (Fig. 7, junctions 3, 4)

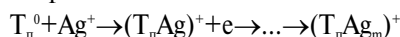


Holes concentration in the region of space charge of silver azide in comparison with their concentration in unirradiated azide will increase. The increase of holes concentration in space charge region of silver azide results in appropriate increase of i_{ph} and V_{ph} by the reaction of nitrogen formation accepted for photolysis of heavy metal azides:



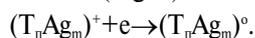
where V_a^+ and V_k^- are the anionic and cation vacancy.

Photolytic silver is formed simultaneously with nitrogen extraction at $AgN_3(A_i)$ photolysis. Formation of photolytic silver particles, in our opinion, occurs at PSES participation

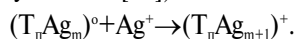


The observed decrease of V_{ph} and i_{ph} at the initial part (I) of kinetic curves in the process and after samples exposure (Fig. 4) confirms the irreversible consumption of surface centers. In growth process of photolytic metal particles the micro-heterogeneous systems silver azide – silver (the product of photolysis) are formed.

Pairs of carriers generated in the region of surface charge of silver azide are redistributed in contact field, formed due to unconformity between thermionic work functions of silver azide and photolytic silver, with transition of nonequilibrium electrons from $AgN_3(A_i)$ conduction band into metal (Fig. 7)



Holes photoemission from photolytic silver into silver azide valence band occurs simultaneously (Fig. 6, junction 2). These processes result, first of all, in growth of holes concentration and, as a result, V_{ph} and i_{ph} increase (area III); secondly, they may stimulate the diffusion of interstitial silver ions to growing particles (silver azide is disordered by Frenkel [21])



In this case, U_{ph} of positive sign from the side of silver azide is formed (Fig. 3), which may promote further

increase of particles size. At light influence on heterosystems $AgN_3(A_i) - Ag$ from the long-wave area of spectrum the holes photoemission from metal into valence band of silver azide occurs (Fig. 6, junction 2). It results in U_{ph} , V_{ph} and i_{ph} occurrence in preliminarily photodecomposed preparations in the long-wave region of spectrum. The uncovered regularities of silver azide photosensitivity changes by photolytic silver in the long-wave spectrum area are conformed to the stated. Indeed, U_{ph} of positive sign from the side of silver azide is formed (Fig. 3). Energy position of U_{ph} , V_{ph} and i_{ph} long-wave threshold for $AgN_3(A_i) - Ag$ heterosystems coincides satisfactorily with the value of energy barrier for holes transition from metal into valence band of silver azide (Fig. 6, junction 2).

To determine the limit stage of photolysis process the time during which the mobile interstitial silver cation (Ag^+) neutralizes localized electron or diffuses to the neutral centre ($T_n Ag_m$)⁰ was estimated. Relaxation time by drift mechanism of mobile cations in the Coulomb field to the localized electron equals the Maxwell relaxation time [22]

$$\tau_i = \varepsilon / 4\pi\sigma,$$

where ε is the inductive capacity ($\varepsilon_{AgN_3(A_i)} = 4$ [23]), σ is the specific conductivity at 293 K ($\sigma_{AgN_3(A_i)} \approx 1 \cdot 10^{-12} \text{ Ohm}^{-1} \cdot \text{sm}^{-1}$ [21]), $\tau_i \approx 0,35$ s. Rate constant of photolysis in this case is $k^I \approx 2,85 \text{ s}^{-1}$.

Average relaxation time at diffusion process behavior may be estimated [22]

$$\tau_0 = e^2 / \sigma k_b a T,$$

where e is the electron charge; a is the lattice constant ($a_{AgN_3(A_i)} = 5.6 \cdot 10^{-8} \text{ sm}$); $T = 293 \text{ K}$, k_b is the Boltzmann constant. At $T = 293 \text{ K}$ $\tau_0 \approx 114$ s. Rate constant of photolysis (k^{II}) in this case is $k^{II} \approx 8,9 \cdot 10^{-3} \text{ s}^{-1}$. The satisfactory coincidence of rate constants of photolysis (Table 2) with k^{II} allows supposing that the limit stage of $AgN_3(A_i)$ photolysis process is diffusion of interstitial silver cation to the neutral centre ($T_n Ag_m$)⁰.

The paper is supported by the grant of the President of RF for assistance of leading scientific schools SS -20.2003.3.

REFERENCES

1. Yang D. Kinetics of solids decomposition. – Moscow: Mir, 1969. – 263 p.
2. Evans B.L., Yoffe A.D. Structure and stability of inorganic azides. II. Some physical and optical properties and the fast decomposition of solid monovalent inorganic azides // Proc. Roy. Soc. – 1959. – V. A250. – P. 364–366.
3. Deb S.K. Optical absorption spectra of azides // Trans. Farad. Soc. – 1969. – V. 65. – P. 3187–3194.
4. Verneker V.R.P. Photodecomposition of Solid Metal Azides // J. Phys. Chem. – 1968. – V. 72. – № 5. – P. 1733–1736.
5. Saveliev G.G., Gavrischenko Yu.V., Zakharov Yu.A. Photo-emf in lead and silver azides // Ivestiya Vusov. Phisika. – 1968. – № 7. – P. 2–4.
6. Surovoy E.P., Bugerko L.N., Rasmatoва S.V. Investigation of kinetic regularities of products formation in the photolysis process of lead azides // Bulletin of Tomsk Polytechnic University. – 2005. – V. 308. – № 1. – P. 93–97.
7. Surovoy E.P., Zakharov Yu.A., Bugerko L.N., Shurygina L.I. Autocatalysis of thallium azide photolysis // High Energy Chemistry. – 1999. – V. 33. – № 5. – P. 387–390.
8. Surovoy E.P., Shurygina L.I., Bugerko L.N. Regularities of micro-heterogeneous systems formation at thallium azide photolysis // Physical Chemistry. – 2003. – V. 22. – № 9. – P. 24–28.
9. Surovoy E.P., Sirik S.M., Bugerko L.N. Photolysis of systems silver-copper azide // Bulletin of the Tomsk Polytechnic University. – 2006. – V. 309. – № 2. – P. 164–169.
10. Vlasov A.P., Surovoy E.P. Photoelectrical sensitivity of heterosystems thallium azide- aluminum in radiation field // Russ. J. Phys. Chem.. – 1991. – V. 65. – № 6. – P. 1465–1469.
11. Surovoy E.P., Sirik S.M., Bugerko L.N. Kinetic of photolysis of heterosystems silver azide with cadmium telluride and copper oxide // Russ. J. Phys. Chem. – 2000. – V. 74. – № 5. – P. 927–933.
12. Surovoy E.P., Bugerko L.N., Rasmatoва S.V. Photolysis of heterosystems «lead azide – cadmium» // Bulletin of Tomsk Polytechnic University. – 2004. – V. 307. – № 2. – P. 95–99.

13. Surovoy E.P., Shurygina L.I., Bugerko L.N. Photolysis of heterosystems thallium azide-metal // Physical chemistry. – 2001. – V. 20. – № 12. – P. 15–22.
14. Surovoy E.P., Bugerko L.N. Thermostimulated gas release from the systems silver azide-metal // Physical chemistry. – 2002. – V. 21. – № 7. – P. 74–78.
15. Surovoy E.P., Bugerko L.N., Zakharov Yu.A., Rasmatoва S.V. Regularities of solid phase product formation of photolysis of heterosystems lead azide-metal // Materialovedenie. – 2002. – № 9. – P. 27–33.
16. A.s. 1325332 USSR. ICI G01N 21/55. The device for measurement reflectance spectra in vacuum / A.I. Turova, G.P. Adushev, E.P. Surovoy et al. Reported 10.11.1985; Published 24.07.1987, Bull. № 27. – 5 p.: ill.
17. Surovoy E.P., Bugerko L.N., Rasmatoва S.V. Photolysis of lead azide in contact with copper oxide (I) // Bulletin of the Tomsk Polytechnic University. – 2006. – V. 309. – № 4. – P. 90–95.
18. Surovoy E.P., Bugerko L.N., Rasmatoва S.V. Photolysis of systems «lead azide – cadmium telluride» // Bulletin of the Tomsk Polytechnic University. – 2004. – V. 307. – № 4. – P. 85–88.
19. Surovoy E.P., Titov I.V., Bugerko L.N. Contact potential difference for lead, silver and thallium azides // Bulletin of the Tomsk Polytechnic University. – 2005. – V. 308. – № 2. – P. 79–83.
20. Kolesnikov L.V. Spectra of energy state and some peculiarities of decomposition reaction of heavy metal azides: Abstract of a thesis ... of a cand. of chemical science. – Minsk, BSU, 1978. – 21 p.
21. Zakharov Yu.A., Gasmaev V.K., Kolesnikov L.V. About the mechanism of nucleation process at thermal decomposition of silver azides // Russ. J. Phys. Chem. – 1976. – V. 50. – № 7. – P. 1669–1673.
22. Meyklyar P.V. Physical processes at formation of latent photographic image. – Moscow: Nauka, 1972. – 399 p.

Received on 08.12.2006

UDC 541.16:182

PASSIVATION OF METAL NANOPOWDERS OBTAINED BY ELECTRIC EXPLOSION OF SEMICONDUCTORS

M.I. Lerner, V.V. Shimanskiy, G.G. Saveliev

SD RAS Institute of Physics of Strength and Material Science, Tomsk

*Tomsk Polytechnic University

E-mail: evp@mail.tomsknet.ru

The influence of composition and gas flow rate at passivation on content of unoxidized metal, particle size and temperature on the metal nanopowder layer obtained by the method of semiconductor electric explosion has been studied. It is shown that the time of forced passivation can be tens times less in comparison with passivation at spontaneous gas diffusion in powder layer.

1. Introduction

Storage and use of metal nanopowders cause a number of specific problems, connected with their high activity. Finely dispersed powders oxidize appreciably at their contact with air. Heat released in the process of oxidation without sufficient heat removal (powders in freely poured condition have a low heat conductivity) may result in metal self-heating and further sintering or powder inflammation.

All stated processes are inherent to full extent in metal nanopowders, produced by the method of electric explosion of conductors (EEC). As the investigations of the process of presintering show [1], the initial sintering temperature of some EEC conforms to ~30 °C. Therefore, it is urgent to ascertain the regularities of passivation process, allowing for decrease of the passivation time and determination of its optimal parameters for storage powders properties (amount of active metal).

On the other hand, the importance of the problems, connected with powder passivation by means of just oxygen containing atmosphere, is defined by the fact that the significant part of existing techniques of metal powder recycling is meant for a definite (usually not large) content of oxide phases.

Change in properties of Cu and Ni powders with average number particle size of 60 nm at their air storage is studied in the paper [2]. It was stated that nickel powders oxidation process lasts 90...100 days, and copper oxidation process lasts 280 days. According to the data of the paper [3], powder apparent density obtained by the method of EEC increases at their storage as the result of desorption and oxidation processes, attaining constant value in ~100 days. In the paper [4] it is shown that the process of aluminium powders oxidation proceeds during ~12 days.

The aim of the given paper is the investigation of the influence of gas mixture flow rate, as well as oxygen and water vapors concentration in gas on nanopowder oxidation that is necessary for the development of methods of passivation time decrease.

2. Experimental technique

Production of nanopowders by the method of EEC to decrease their activity the spontaneous passivation by air is usually applied – see, for example [3–6]. In this case, a container with nanopowder, obtained in the atmosphere Ar, is filled through a small regulated hole spontaneously with air, which diffuses through the layer of argon, being over the powder, and then into the layer